Colloid and Polymer Science (2018) 296:1609–1613
https://doi.org/10.1007/s00396-018-4373-0

SHORT COMMUNICATION

Enhanced magnetorheological performance of carbonyl iron/natural rubber composite elastomer with gamma-ferrite additive

Chul Joo Lee [1] · Seung Hyuk Kwon [1] · Hyoung Jin Choi [1] · Kyung Ho Chung [2] · Jae Heum Jung [3]

Received: 23 May 2018 / Revised: 6 July 2018 / Accepted: 8 July 2018 / Published online: 23 July 2018

Abstract

Magnetorheological (MR) elastomers have attracted considerable attention for their potential applications but their MR efficiency requires significant improvement before they can be used commercially. In this study, rod-shaped hard magnetic gamma-ferrite (γ-Fe_2O_3) nanoparticles were added to a carbonyl iron (CI)@natural rubber (NR) composite elastomer to enhance the MR effect of CI-based MR elastomers. The surface morphological state of the dispersed magnetic particles was tested using scanning electron microscopy, and the fracture profiles of the MR elastomers made of magnetic particles were observed to be anisotropically aligned by mapping using energy dispersive X-ray spectroscopy. MR properties of the MR elastomers based on pure CI and CI@ γ-Fe_2O_3 were examined using a rotational rheometer under different magnetic field strengths with an enhanced MR efficiency of about 25%.

Keywords Ferrite · Additive · Carbonyl iron · Natural rubber · Magnetorheological elastomer

Introduction

Magnetorheological (MR) materials, such as MR fluids [1, 2], have been recognized for their ability as smart and intelligent materials with easy conversion between a liquid-like and solid-like state within a very short time under a magnetic field. Although the properties of MR fluids are controlled by the shear viscosity and yield stress, the properties of MR elastomers are controlled by the modulus according to the external magnetic field [3, 4]. MR elastomers can overcome the problems of sealing and particle settling by mixing the magnetic particles in a solid matrix, such as natural rubber, silicone rubber, and polyurethane [5–8]. Because of these characteristics, MR elastomers have a range of engineering applications, including electromagnetic shielding, 3D printing, rolling friction controllers, and engine mounts in automobiles [9–11].

✉ Hyoung Jin Choi
hjchoi@inha.ac.kr

1 Department of Polymer Science and Engineering, Inha University, Incheon 22212, South Korea

2 Department of Polymer Engineering, University of Suwon, Hwaseong 445-743, South Korea

3 Materials Development Team, Daeheung Rubber & Technology Co., Kimhae 621-884, South Korea

Among the various soft magnetic particles for MR elastomers, such as carbonyl iron (CI), ferrite, and nickel particles [12, 13], CI is a representative MR material owing to its soft magnetic features, appropriate size, and high magnetic permeability [14]. In addition, while different materials involving carbon nanotubes, nickel-zinc ferrite, and polyaniline [15–17], have been applied as additives to improve the dispersion stability of MR fluids, the MR effect is reduced in many cases. On the other hand, the introduction of a hard magnet particle as an additive can increase both the dispersion stability and MR effect for MR fluids. In particular, gamma-ferrite (γ-Fe_2O_3) particles were found to be advantageous for improving the MR effect by broadening the contact surface in the formation of a chain in a rod-like shape [18].

In this study, rod-shaped hard magnetic γ-Fe_2O_3 particles were used as an additive in a CI particle-based natural rubber (NR) composite MR elastomer to improve the MR efficiency of CI-based MR elastomers in Fig. 1. A magnetic field was applied in one direction during fabrication to produce anisotropic MR elastomers with uniformly aligned magnetic particles for improving MR and dielectric properties [19]. The morphology of the particles and the alignment of the MR elastomer were confirmed by scanning electron microscopy (SEM), and their rheological properties were measured and analyzed using a rotational rheometer.

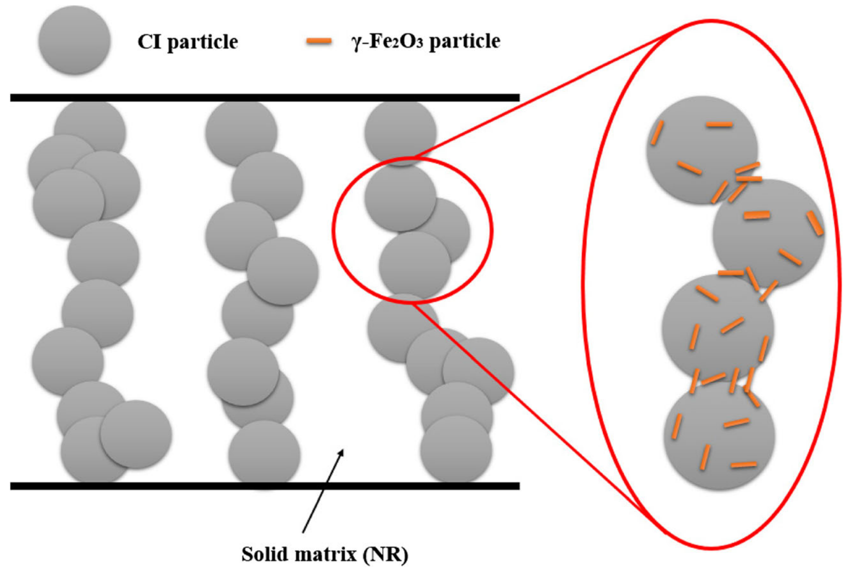

Fig. 1 Schematic diagram of additive system of CI particles with γ-Fe_2O_3 particles

Materials and synthesis method

Materials

CI (Standard CC-grade, BASF, Germany) particles with a density of 7.8 g/cm^3 and 2 wt% rod-shaped γ-Fe_2O_3 (HR-350, Magnox) particles with a density of 4.7 g/cm^3 were used as magnetic substances. Natural rubber (NR) (CV-60) was used as solid matrix, and carbon black (CB) (N990, Cancarb, Canada) was added as both filler and hardening agent.

Preparation of CI@ γ-Fe_2O_3-based MR elastomer

Pure CI and 2 wt% rod-shaped γ-Fe_2O_3 particles were mixed evenly. Natural rubber (NR) of 100 phr, CI@ γ-Fe_2O_3 particles of 200 phr, and carbon black (CB) of 20 phr were mixed using a general rubber mixing machine (Banbury mixer, HYB-3L, Hyupyoung machinery Co., Korea) for 15 min. Subsequently, this composite rubber was placed into a 1-mm circle-shaped mold and heated to 160 °C for 10 min using customized heat-magnet coupled equipment under a pressure of 10 Mpa and a magnetic field intensity of 840 mT. Finally, the MR elastomer containing CI@ γ-Fe_2O_3 particles aligned along a uniform direction was fabricated.

Characterization

The morphology of the CI@ γ-Fe_2O_3 particles and mapping images of the fractured surfaces of the MR elastomer were examined by high-resolution SEM (HR-SEM) (SU8010, Hitachi, Japan) and energy dispersive X-ray spectroscopy (EDX), respectively, with a high accelerating voltage of approximately 15 kV. Note that the EDX was to examine alignment of the dispersed magnetic particles through its mapping focusing on the Fe element in the magnetic particles. The MR characteristics of the MR elastomers based on both CI and CI@ γ-Fe_2O_3 were confirmed using a rotational rheometer (MCR 300, Anton Paar, Austria) with a high voltage generator and special geometry (PP20/MRD/TI/S) with a sand-blasted surface to prevent a potential slip phenomenon because the MR elastomeric sample disc slips easily between the two plates.

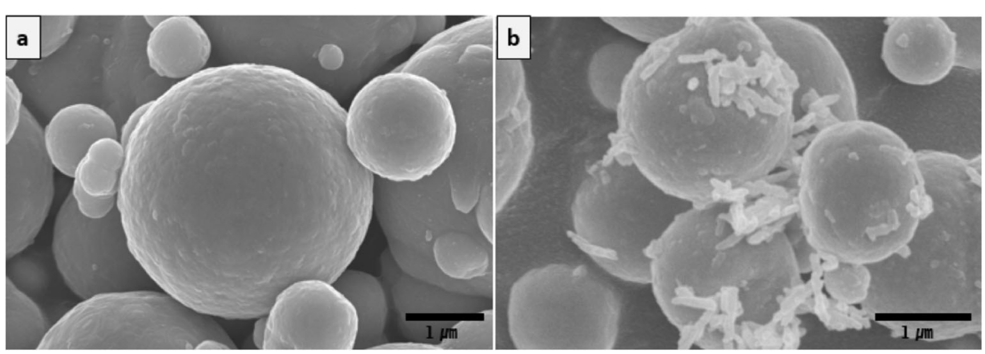

Fig. 2 SEM images of pure CI (a) and CI@ γ-Fe_2O_3 particles

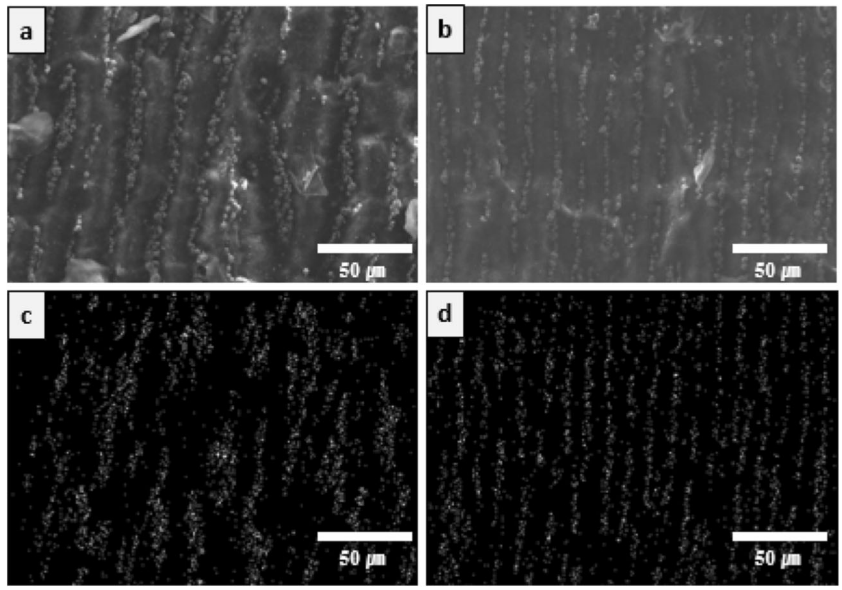

Fig. 3 Fractography and mapping images of **a, c** pure CI- and **b, d** CI@ γ-Fe_2O_3-based anisotropic MR elastomer

Results and discussion

Figure 2 represents SEM images of the pristine CI (a) and CI@ γ- Fe_2O_3 (b) particles, in which the surface of pure CI appears smooth with an almost spherical shape and a size of 1–4 μm. On the other hand, the CI@γ-Fe_2O_3 particles contained rod-shaped γ-Fe_2O_3 particles on not only the surface of the CI particles, but also in the empty space among the CI microspheres because of the magnetic interaction of the hard magnetic γ-Fe_2O_3 particles. Therefore, when the CI particles form a chain under an applied magnetic field, higher MR performance can be expected because γ-Fe_2O_3 particles act as a support among CI particles [18].

To examine aligned magnetic particles of the MR elastomers, a MR elastomer sample was placed in liquid nitrogen, frozen, and then broken to produce a smooth fracture surface. Figure.3a, b presents images of the fractured surface profiles of both the CI and γ-Fe_2O_3 particle-based MR elastomers confirmed by HR-SEM. Furthermore, the Fe components in the samples were more distinctively mapped by EDX to exhibit the alignment of magnetic particles in each anisotropically prepared MR elastomer (as shown in Fig. 3c, d). In the case of a CI-based MR elastomer, the CI particles were aligned like fibrillar chains [20], but they were discontinuous and irregular. In contrast, the MR elastomer based on CI@ γ-Fe_2O_3 particles showed an almost parallel chain structure that was regular and continuous because the added γ-Fe_2O_3 particles were located in the empty spaces among the CI particles to support and stabilize the chain. These results suggest that the CI@ γ-Fe_2O_3-based MR elastomer will have a higher modulus and efficiency than the CI-based MR elastomer. Note that while various additives including carbon nanotube increase dynamic

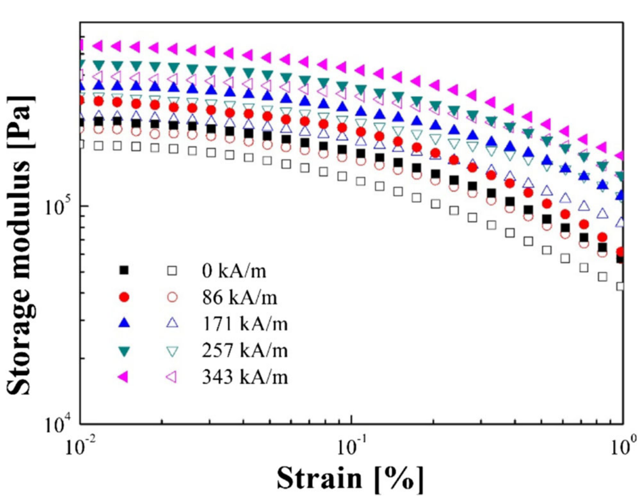

Fig. 4 Storage moduli of MR elastomers based on pure CI (open) and CI@ γ-Fe_2O_3 (closed) as a function of strain under a variety of magnetic field strengths

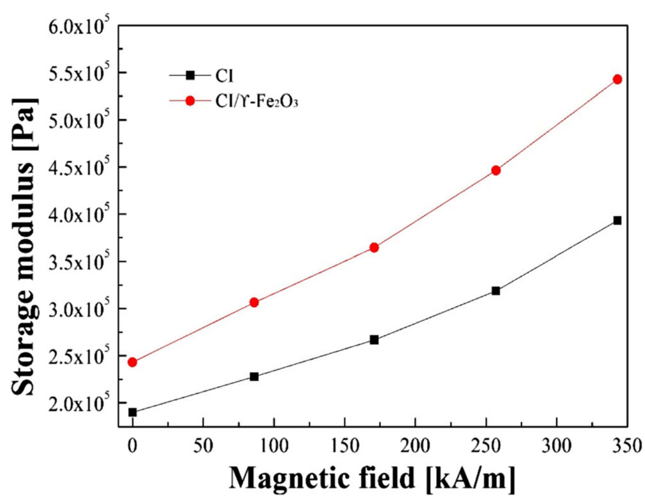

Fig. 5 The tendency of storage modulus of anisotropic MR elastomer based on CI (square) and CI@ γ-Fe_2O_3 (circle) under different magnetic field strengths

stiffness and loss factor of CI-based MR elastomers, its addition was found to reduce the MR effect [21].

Figure 4 shows storage modulus of the samples as a function of shear strain from the strain amplitude sweep test, demonstrating the viscoelastic characteristics for both CI-based (open) and CI@ γ-Fe_2O_3-based (closed) MR elastomers. This test was conducted at a fixed frequency of 1 Hz, varying the strain from 0.01 to 1%. Overall, the storage modulus of the MR elastomer based on CI@ γ-Fe_2O_3 was higher than those of the CI-based MR elastomer under an applied external magnetic field. Moreover, the storage modulus tended to decrease with increasing strain and increase with increasing magnetic field strength [22]. The linear viscoelastic (LVE) region, where the storage modulus remained constant before a sharp decrease, appeared at a low strain region because the parallel chain structures were maintained in this region under the influence of an external magnetic field. In addition, the storage modulus was also independent in this LVE region.

Figure 5 demonstrates the relationship between storage modulus and strain under a variety of strains at a constant angular frequency of approximately 6.28 rad/s. The storage moduli of the two MR elastomer samples were proportional to the magnetic field strength, and the slope tended to increase with increasing magnetic field. On the other hand, the slope of the CI@γ-Fe_2O_3-based MR elastomer increased sharply with increasing magnetic field intensity compared to the slope of the CI-based MR elastomer [23]. This suggests that γ-Fe_2O_3 particles have a higher storage modulus because of the formation of a stable chain. Note that in the case of silicon rubber matrix, poly(trimethylsilyloxyethyl methacrylate)-coated CI particles with improved wettability and dispersibility showed enhanced MR efficiency [24], and the issue on affinity between CI particles and elastomer matrix could be also important [25].

Conclusion

A CI@ γ-Fe_2O_3-based MR elastomer was fabricated by adding γ-Fe_2O_3 nanoparticles as an additive and the behaviors were compared with those of a pure CI-based MR elastomer. Mapping showed that the CI@ γ-Fe_2O_3-based MR elastomer was aligned more uniformly than the CI-based MR elastomer. Moreover, the strain sweep test confirmed that the CI@ γ-Fe_2O_3-based MR elastomer had a higher modulus. The modulus increased significantly with increasing magnetic field strength.

Funding information This work was financially supported by the Ministry of Trade, Industry & Energy, Korea (#10047791).

Compliance with ethical standards

Conflict of interest The authors declare that they have no conflict of interest.

References

1. Mrlik M, Ilcikova M, Sedlacik M, Mosnacek J, Peer P, Filip P (2014) Cholesteryl-coated carbonyl iron particles with improved anti-corrosion stability and their viscoelastic behaviour under magnetic field. Colloid Polym Sci 292:2137–2143
2. Wang G, Ma Y, Tong Y, Dong X (2016) Synthesis, characterization and magnetorheological study of 3-aminopropyltriethoxysilane-modified Fe_3O_4 nanoparticles. Smart Mater Struct 25:035028
3. Siegfried P, Koo JH, Pechan M (2014) Torque characterization of functional magnetic polymers using torque magnetometry. Polym Test 37:6–11
4. Wen Q, Wang Y, Gong X (2017) The magnetic field dependent dynamic properties of magnetorheological elastomers based on hard magnetic particles. Smart Mater Struct 26:075012
5. Bellucci FS, de Almeida FCL, Nobre MAL, Rodriguez-perez MA, Paschoalini AT, Job AE (2016) Magnetic properties of vulcanized natural rubber nanocomposites as a function of the concentration, size and shape of the magnetic fillers. Composites Part B 85:196–206
6. Bunoiu M, Bica I (2016) Magnetorheological elastomer based on silicone rubber, carbonyl iron and Rochelle salt: effects of alternating electric and static magnetic fields intensities. J Ind Eng Chem 37:312–318
7. Sasaki S, Tsujiei Y, Kawai M, Mitsumata T (2017) Electric conductivity and dielectric-breakdown behavior for polyurethane magnetic elastomers. J Phys Chem B 121:1740–1747
8. Li WH, Zhou Y, Tian TF (2010) Viscoelastic properties of MR elastomers under harmonic loading. Rheol Acta 49:733–740
9. Sedlacik M, Mrlik M, Babayan V, Pavlinek V (2016) Magnetorheological elastomers with efficient electromagnetic shielding. Compos Struct 135:199–204
10. Bastola AK, Hoang VT, Li L (2017) A novel hybrid magnetorheological elastomer developed by 3D printing. Mater Des 114:391–397
11. Lian CL, Lee KH, Lee CH (2017) Application study of magnetorheological elastomer to rolling friction control. J Tribol 139(5):051101
12. Malini KA, Mohammed EM, Sindhu S, Joy PA, Date SK, Kulkarni SD, Kurian P, Anantharaman MR (2001) Magnetic and processability studies on rubber ferrite composites based on natural rubber and mixed ferrite. J Mater Sci 36:5551–5557
13. Landa RA, Antonel PS, Ruiz MM, Perez OE, Butera A, Jorge G, Oliveira CLP, Negri RM (2013) Magnetic and elastic anisotropy in magnetorheological elastomers using nickel-based nanoparticles and nanochains. J Appl Phys 114:213912
14. Kim SY, Kwon SH, Liu YD, Lee JS, You CY, Choi HJ (2014) Core–shell-structured cross-linked poly(glycidyl methacrylate) coated carbonyl iron microspheres and their magnetorheology. J Mater Sci 49:1345–1352
15. Fang FF, Jang IB, Choi HJ (2007) Single-walled carbon nanotube added carbonyl iron suspension and its magnetorheology. Diam Relat Mater 16:1167–1169
16. Hajailou A, Mazlan SA, Shila ST (2016) Magnetic carbonyl iron suspension with Ni-Zn ferrite additive and its magnetorheological properties. Mater Lett 181:196–199
17. Sedlacik M, Pavlinek B, Saha P, Svrcinova P, Filip P, Stejskal J (2010) Rheological properties of magnetorheological suspensions based on core–shell structured polyaniline-coated carbonyl iron particles. Smart Mater Struct 19:115008
18. Jang DS, Liu YD, Kim JH, Choi HJ (2015) Enhanced magnetorheology of soft magnetic carbonyl iron suspension with hard magnetic γ-Fe_2O_3 nanoparticle additive. Colloid Polym Sci 293:641–647

19. Moucka R, Sedlacik M, Cvek M (2018) Dielectric properties of magnetorheological elastomers with different microstructure. Appl Phys Lett 112:122901
20. Rudykh S, Bertoldi K (2013) Stability of anisotropic magnetorheological elastomers in finite deformations: a micromechanical approach. J Mech Phys Solids 61:949–967
21. Poojary UR, Hegde S, Gangadharan KV (2018) Experimental investigation on the effect of carbon nanotube additive on the field-induced viscoelastic properties of magnetorheological elastomer. J Mater Sci 53:4229–4241
22. Yunus NA, Mazlan SA, Ubaidillah ASAA, Khairi MHA, Wahab NAA, Shilan SY (2016) Investigation on magnetic field dependent modulus of epoxidized natural rubber based magnetorheological elastomer. J Phy Conf Ser 776:012024
23. Jung HS, Kwon SH, Choi HJ, Jung JH, Kim YG (2016) Magnetic carbonyl iron/natural rubber composite elastomer and its magnetorheology. Compos Struct 136:106–112
24. Cvek M, Mrlik M, Ilcikova M, Mosnacek J, Munster L, Pavlinek V (2016) Synthesis of silicone elastomers containing silyl-based polymer-grafted carbonyl iron particles: an efficient way to improve magnetorheological, damping, and sensing performances. Macromolecules 50:2189–2200
25. Wang Y, Zhang X, Chung K, Liu C, Choi SB, Choi HJ (2016) Formation of core–shell structured complex microparticles during fabrication of magnetorheological elastomers and their magnetorheological behavior. Smart Mater Struct 25:115028